PCCP

Accepted Manuscript

ROYAL SOCIETY OF CHEMISTRY

www.rsc.org/pccp

Internal Electric Fields in Small Water Clusters [$(H_2O)_n$; n=2-6]

Saumik Sen,‡*[a] B. Manjusha,‡[a] S. Venkat Lata[a] and G. Naresh Patwari*[a]

[a] Department of Chemistry, Indian Institute of Technology Bombay, Powai, Mumbai 400076 India

E-mail: saumiksen@chem.iitb.ac.in; naresh@chem.iitb.ac.in

‡These authors contributed equally

12 **TOC Graphic**

The stabilization energies and the average red-shifts in the O–H stretching frequencies in the water clusters correlate linearly with the electric field derived from the molecular electrostatic potential.

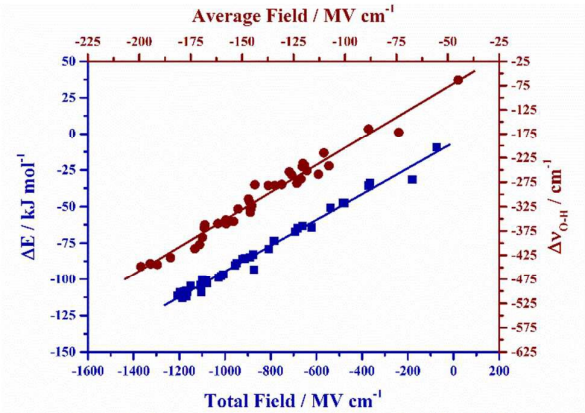

13

Abstract

The electric field experienced by a water molecule within a water cluster depends on its position relative to the rest of the water molecules. The stabilization energies and the red-shifts in the donor O–H stretching vibrations in the water clusters increase with the cluster size which is concomitant with the increase in the electric field experienced by the donor O–H of a particular water molecule due to the hydrogen bonding network. The red-shifts in O–H stretching frequencies show a spread of about ± 100 cm^{-1} against the corresponding electric fields. Deviations from linearity were marked in the region of 100 - 160 MV cm^{-1}, which can be attributed to the strain in the hydrogen bonding network, especially structures with DDAA and DDA motifs. The linear Stark effect holds up to 200 MV cm^{-1} of internal electric field for the average red-shifts in the O–H stretching frequencies, with Stark tuning rate of 2.4 cm^{-1}/(MV cm^{-1}), suggests the validity of the classical model in small water clusters.

1. Introduction

Understanding hydrogen bonding has been a subject of investigation starting from the landmark article by Latimer and Rodebush in 1920,[1] where they have proposed the concept of hydrogen bonding in water. Ever since, large numbers of reports have explored the hydrogen bonding in water. Based on the bottom-up approach, water clusters have been used to model the structure, dynamics and the cooperative effects of hydrogen bonding.[2] Numerous theoretical reports in the literature address the structures, energetics, morphology and various properties such as dipole moments, polarizabilities of small water clusters [$(H_2O)_n$; n=2-6].[3] On the experimental front, IR spectroscopy has been widely used to investigate water clusters and the experimentally observed spectra could be assigned to some of the low energy structures predicted by theoretical calculations.[4] More recently, the dissociation energies of the water –dimer and –trimer have been reported, which are in good agreement with the calculated stabilization energies.[5]

An alternate, but an exceedingly effective way to understand the hydrogen bonding in water clusters is by evaluating the electric field experienced by a particular water molecule due to the rest of the water molecules that make up the cluster. More importantly, the electric field experienced by a particular water molecule will depend on its environment and thus reports the local structure around the water molecule in question.[6] Boxer and co-workers have established that the electric field experienced by a molecule due to its environment can be experimentally measured using vibrational Stark spectroscopy.[6] Further, it was also shown for several hydrogen-bonded systems that the shift in the donor (X–H; X = O, N, S) stretching frequency is proportional to the electric field experienced by the X–H bond due to the hydrogen bond acceptor.[7] In this work we

evaluate the electric field experienced by each of the hydrogen-bonded O–H groups in a water cluster. An attempt is made to correlate the electric fields with the stabilization energies of the water cluster and rationalize the vibrational frequency shifts.

2. Computational Methods

To begin with, structures of small water clusters [$(H_2O)_n$; n = 2-6] were optimized using MP2/aug-cc-pVDZ and B3LYP/6-311++G(*d,p*) levels of theory using GAUSSIAN-09 [8] with its graphical interface GaussView 5.[9] The geometry optimization of various structures of the tetramer, pentamer and the hexamer was carried out starting from the coordinates reported earlier for these structures.[3e,g,h] Frequency calculations followed the geometry optimization at the same level of theory to evaluate the zero-point energies and the vibrational frequencies of the systems, and to ensure that all the structures correspond to true minima. The calculated stabilization energies were corrected for the vibrational zero-point energy (ZPE) and the basis-set superposition error (BSSE) using counterpoise method. The BSSE correction was made after geometry optimization. The stabilization energy for all the water clusters was calculated as the difference between the energy of *n*-water cluster and energy of *n* water molecules.

To account for the effect of charge distribution on the stabilization energies and the shifts in the O–H stretching frequencies in the water clusters electric field calculations were carried out using the procedure laid out by Boxer and co-workers.[7] To calculate the electric field on a specific OH group of a water molecule in the hydrogen-bonded network the O and H atoms were replaced with ghost atoms and the second H atom was removed. Following this, the molecular electrostatic potential (MESP) arising from the hydrogen bond acceptor was calculated at the position of O and H atoms of the

hydrogen bond donor. The MESP on the atom O/H located at the position $\vec{R}_{\mathrm{O}} / \vec{R}_{\mathrm{H}}$ is given by the equation (1),[10]

$$V_{\mathrm{O/H}} = \sum_{\mathrm{A} \neq \mathrm{O,H}} \frac{Z_{\mathrm{A}}}{|\vec{R}_{\mathrm{A}} - \vec{R}_{\mathrm{O/H}}|} - \int \frac{\rho(\vec{r}) d^3\vec{r}}{|\vec{r} - \vec{R}_{\mathrm{O/H}}|} \tag{1}$$

where Z_{A} is the nuclear charge of atom A located at $\vec{R}_{\mathrm{A}}$ and $\rho(\vec{r})$ is the electron density of the molecule and $\vec{r}$ is a dummy integration variable. The projection of electric field onto the bond was calculated as the gradient of the electrostatic potential along the bond axis along O$\rightarrow$H direction, which is given by the equation (2)

$$\vec{F} = -\nabla V = \frac{-\left(V_{\mathrm{O}} - V_{\mathrm{H}}\right)}{\left|\left(\vec{R}_{\mathrm{O}} - \vec{R}_{\mathrm{H}}\right)\right|} \tag{2}$$

In the equation (2) V_{O} and V_{H} are the measure of the electrostatic potential at the position of atoms O and H due to all the electrons and rest of the nuclei in the system of interest. For the hydrogen-bonded water clusters, starting from the optimized geometry, each donor O–H group was sequentially replaced with the dummy atoms and the MESP potential was calculated at the positions of O and H atoms using both MP2/aug-cc-pVDZ and B3LYP/6-311++G(*d,p*) levels of theory. MESP at atom centres were obtained from the standard output of *GAUSSIAN-09*.[8] The projection of the electric field was calculated on each of the donor O–H groups in the hydrogen-bonded water clusters with number of water molecules ranging from two (dimer) to six (hexamer).

3. Results and Discussion

The optimized structures water –dimer, –trimer, –tetramer and –pentamer are shown in Fig. 1 at both MP2/aug-cc-pVDZ and B3LYP/6-311++G(*d,p*) levels of theory. A single stable structure was found for the water–dimer and two for water–trimer. In the case of

water–tetramer, six structures were obtained at the MP2 level, while seven structures were obtained at the B3LYP level. For the water–pentamer the number of structures obtained at the MP2 and the B3LYP levels are eight and thirteen, respectively. Fig. 2 shows the optimized structures of the water–hexamer. In this case a total of thirty structures were obtained, with twenty-three structures at the MP2 level and twenty-five at the B3LYP level. Cumulatively, forty structures were obtained at MP2 level and forty-eight structures were obtained at the B3LYP level. Table 1 lists the vibrational zero-point energy (ZPE) and the basis-set superposition error (BSSE) corrected stabilization energy for all the water clusters shown in Figs. 1 and 2. The stabilization energies calculated at the B3LYP level were on the average 14% higher than the corresponding MP2 values (see Fig. S1; ESI). At MP2/aug-cc-pVDZ level the water–dimer and –trimer are stabilized by 9.7 and 35.8 kJ mol^{-1}, respectively (see Table 1). In comparison, the corresponding experimentally determined dissociation energies are 13.2 and 31.7 kJ $mo1^{-1}$.[5] Therefore, the present method underestimates the stabilization energy of the water-dimer and overestimates the stabilization energy of the water-trimer.

The stable water–dimer, W2, is a single hydrogen-bonded structure and the electric field along the donor O–H group at the MP2 level was calculated as -73.79 MV cm^{-1}. On the other hand, the lowest energy structure of water–trimer, W3_1, is a cyclic structure with C_1 symmetry. In this case the electric field along the three donor O–H groups were calculated as -124.07, -123.76 and -122.08 MV cm^{-1} (at the MP2 level; see Table S1). The differences in the electric field of the three donor O–H groups are very marginal. The total (cumulative) electric field, $\Sigma\vec{F}$, experienced by hydrogen bonding network of W3_1 water–trimer is the sum of the electric fields along the three individual donor O–H groups, which is -369.92 MV cm^{-1}. The total electric field experienced by hydrogen bonding network for each of the structures shown in Figs. 1 and 2 is listed in

Table 1. The stabilization energy of water dimer can be attributed to a single O–H···O hydrogen bond. On the other hand, for the W3_1 water–trimer the total stabilization energy is due to three O–H···O hydrogen bonds. Therefore a relationship between total electric field and the stabilization energy is explored by plotting these two quantities in Fig. 3. A straight-line fit to the data points clearly illustrates that the stabilization of the water cluster is directly proportional to the total electric field in the cluster. Calculations using B3LYP/6-311++G(*d,p*) level also yields similar results (see Fig. S2; ESI). Moreover, the plot of average stabilization energy against average electric field also shows a linear correlation, and is shown in Fig. S3 (se ESI). The observed results are in agreement with the linear correlation between the stabilization energies and the electric fields for the π hydrogen-bonded complexes of phenol, indole and thiophenol.[7b]

Contrary to the simpler analysis of the stabilization energies, the analysis of the O–H stretching vibrational frequencies in the water clusters is convoluted due to coupling of the O–H oscillators. While several strategies may be adapted to analyse the O–H stretching vibrations, a simplest model is to segregate the free and the hydrogen-bonded OH groups. For instance, in the case of water–dimer only one O–H group is involved in hydrogen bond formation while the remaining three O–H groups are free. Similarly in the case of W3_1 water–trimer the numbers of O–H groups that are hydrogen-bonded and free are three each. In almost all the cases the free and the hydrogen-bonded O–H stretching frequencies are separated on the frequency scale, with the unscaled free and hydrogen-bonded O–H stretching frequencies typically around 3800 cm^{-1} or higher and 3700 cm^{-1} or lower, respectively, as shown in Table S1 (see ESI). Therefore for a given water cluster an average value of the red-shift in the O–H stretching frequencies, $\overline{\Delta\bar{\nu}_{\text{O-H}}}$, due to formation of hydrogen bonding network can be defined as the difference between the mean of the free, $\overline{\bar{\nu}_{\text{O-H(F)}}}$, and mean of the

hydrogen-bonded, $\overline{\overline{\nu}_{\text{O-H(HB)}}}$, O–H stretching frequencies. An average of electric fields, $\overline{\vec{F}}$, along all the hydrogen-bonded O–H groups for a water cluster can also be evaluated, values of which are also listed in Table S2 (see ESI). Fig. 5 shows the plot of average red-shift in the hydrogen-bonded O–H stretching frequencies, $\overline{\Delta\overline{\nu}_{\text{O-H}}}$, against the average electric field, $\overline{\vec{F}}$, in several water clusters. A linear relationship between $\overline{\Delta\overline{\nu}_{\text{O-H}}}$ and $\overline{\vec{F}}$ is clearly evident from Fig. 4. The slope of the line in Fig. 4 is termed as Stark tuning rate, $\Delta\vec{\mu}$, and is given by the equation (3)[6,7]

$$\overline{\Delta\overline{\nu}} = \Delta\vec{\mu}\cdot\overline{\vec{F}} \qquad (3)$$

which is a measure of the change in the dipole moments in the vibrationally excited state relative to the ground state. Linear fit to the data points in Fig. 4 yields Stark tuning rates of 2.53 $cm^{-1}/(MV\ cm^{-1})$. A similar plot for the values calculated at B3LYP/6-311++G(*d,p*) level calculation (see Fig. S4, ESI) gives the Stark tuning rates of 2.60 $cm^{-1}/(MV\ cm^{-1})$.

In order to decouple the vibrations of the O–H oscillators in the water clusters, all but one hydrogen atoms were replaced with deuterium atoms and the vibrational frequency calculation was carried out. This calculation yields the O–H stretching frequency of a single O–H group in the deuterated water cluster. The O–H stretching frequencies of all the hydrogen-bonded O–H groups in a given cluster, one at a time, were systematically calculated. Similarly one of the hydrogen bonded hydrogen atom was replaced with the deuterium atom and the O–D stretching frequencies of all the hydrogen-bonded O–D groups were calculated. For the 40 structures optimized at MP2/aug-cc-pVDZ level (see Figs. 1 and 2) 249 independent hydrogen bonded O–H / O–D groups were identified. (see Table S1; ESI). The shift in the O–H / O–D stretching frequency is the difference between the corresponding stretching frequencies in the

partially deuterated water (HOD). The results of these calculations are listed in Table S2 (see ESI) and the plots of shifts in the $\Delta\nu_{\text{O-H}}$ and $\Delta\nu_{\text{O-D}}$ against the corresponding electric field are shown in Fig. 5. These plots show considerable spread in the data points with largest spread in the region corresponding to local electric fields of 100 to 160 MV cm^{-1}. A linear fit to the data points in the shaded region with 206 data points (see Fig. S7; ESI) yields a Stark tuning rate of 2.7 cm^{-1}/(MV cm^{-1}). However, the corresponding residuals are within ±100 cm^{-1}. The data points in the electric field regions of 100 to 160 MV cm^{-1} (encircled) show larger deviations. Since the deviations in this region correspond to smaller frequency shifts, these can be attributed to increased anharmonicity for these vibrations. These data points correspond to the water-hexamer structures of W6_3, W6_8, W6_10, W6_11 and several others (see Fig. 2) in which at least one of the OH groups has strained hydrogen bond and is part of the DDAA (double donor double acceptor) or DDA (double donor single acceptor) structural motif. On the other hand the data points above 200 MV cm^{-1} show deviations corresponding to larger frequency shifts, which suggests that the classical model may no longer be adequate.

Fig. 6 shows the average shifts ($\overline{\Delta\bar{\nu}_{\text{O-H/D}}}$) in the O–H and O–D stretching vibrations in each cluster plotted against the average electric field. Once again a linear correlation is observed with Stark tuning rates of 2.41 and 1.76 cm^{-1}/(MV cm^{-1}) for the O–H and O–D stretching vibrations, respectively. The Stark tuning rate for the O–H stretching vibrations obtained by two different methodologies have similar values (2.53 and 2.41 cm^{-1}/(MV cm^{-1})). Interestingly, the Stark tuning rate of 2.6 cm^{-1}/(MV cm^{-1}) was reported for the O–H···π hydrogen-bonded complexes of phenol,[7] and the present values are in close agreement.

One of the significant observations in the present work is the linearity of the average shifts in the O–H stretching vibrations against the local electric fields up to 200

MV cm^{-1}. However, in the case of O–H···π hydrogen-bonded complexes of phenol, it was observed for modest electric fields the red-shifts in the O–H stretching deviate from linearity. The deviations from the linearity in the case of O–H···π hydrogen-bonded complexes of phenol has been attributed to the quadratic Stark effect.[7] On the other hand the C=O stretching frequencies in the ketosteroid isomerase show frequency shift commensurate with the electric fields of up to 150 MV cm^{-1} in water, which includes the solvent field.[6e] The linear correlation of average red-shifts in the O–H stretching vibrations up to 200 MV cm^{-1} clearly suggests the validity of classical model linear Stark effect in small water clusters.

4. Conclusions

The electric field along the hydrogen bond donor O–H group was calculated for several water clusters using molecular electrostatic potentials. Both the stabilization energy and electric field increase with increase in number of hydrogen bonds in a water cluster and the stabilization energy of the water clusters is directly proportional to the sum of the electric fields along all the donor O–H groups. The plot of red-shifts in O–H stretching frequencies against electric fields show a spread of about ±100 cm^{-1} from linearity. Additionally, the data points in the region of 100-160 MV cm^{-1} show larger deviations due to anharmonicity. These data points correspond to strained hydrogen bonds with DDAA and DDA structural motifs. On the other hand the average red-shift in the O–H stretching frequencies of all the O–H···O hydrogen bonds in the water cluster is linearly correlated with the average of all the electric fields on the donor O–H group. The average Stark tuning rate for the O–H group in water clusters is about 2.4 cm^{-1}/(MV cm^{-1}), which is similar to the Stark tuning rate of 2.6 cm^{-1}/(MV cm^{-1}) for the O–H···π hydrogen-bonded complexes of phenol.

Author Contributions

The problem was formulated by GNP and SS. BM carried out most of the calculations with some assistance from SVL. The results were interpreted jointly by GNP and SS along with BM and SVL.

Acknowledgements

This material is based upon work supported by Science and Engineering Research Board of Department of Science and Technology (Grant No. SB/S1/PC-29/2012) to GNP. SS and BM thank IIT Bombay and UGC for their research fellowship, respectively. High performance computing facility of IIT Bombay is gratefully acknowledged. Authors wish to thank Prof. Steven G. Boxer, Dr. Sayan Bagchi and Dr. Debashree Ghosh for the discussions and useful suggestions. Authors also wish to thank the reviewers, whose comments have considerably improved the manuscript.

Notes

Electronic Supplementary Information (ESI) available: List of stabilization energies, total and average electric fields, and unscaled vibrational frequencies of free and hydrogen bonded O−H for all the water clusters. Additionally, comparison of stabilization energies in MP2 and B3LYP level is shown for entire data set of all the water clusters. See DOI: 10.1039/x0xx00000x

References

1 W. M. Latimer and W. H. Rodebush, *J. Am. Chem. Soc.*, 1920, **42**, 1419-1433.

2 (a) W.A.P. Luck, *J. Mol. Str.*, 1998, **448**, 131-142. (b) S. Xantheas, *Chem. Phys.*, 2000, **258**, 225-231. (c) T. James, D. J. Wales and J. Hernández-Rojas, *Chem. Phys. Lett.*, 2005, **415**, 302-307. (d) V. S. Znamenskiy and M. E. Green, *J. Chem. Theory Comput.*, 2007, **3**, 103-114. (e) K. Stokelya, M. G. Mazzaa, H. E. Stanleya, and G. Franzese, *Proc Natl Acad Sci U S A.*, 2010, **107**, 1301-1306. (f) S. Acosta-Gutiérrez, J. Hernández-Rojas, J. Bretón, J. M. G. Llorente and D. J. Wales, *J. Chem. Phys.*,

2011, **135**, 124303-11. (g) X. Liu, W.-C. Lu, C. Z. Wang and K. M. Ho, *Chem. Phys. Lett.*, 2011, **508**, 270-275. (h) T. Morawietz, V. Sharma and J. Behler, *J. Chem. Phys.*, 2012, **136**, 064103-11. (i) R. J. Saykally and D. J. Wales, *Science*, 2012, **336**, 814-815. (j) T. Morawietz and J. Behler, *J. Phys. Chem. A*, 2013, **117**, 7356-7366. (k) L. Albrecht, S. Chowdhury and R. J. Boyd, *J. Phys. Chem. A*, 2013, **117**, 10790-10799. (l) C. Pérez, D. P. Zaleski, N. A. Seifert, B. Temelso, G. C. Shields, Z. Kisiel and B. H. Pate, *Angew. Chem. Int. Ed.*, 2014, **53**, 14368-14372. (m) S. Saha and G. N. Sastry, *Mol. Phys.*, 2015, **113**, 3031-3041.

3 (a) S. S. Xantheas and T. H. Dunning Jr. *J. Chem. Phys.*, 1993, **99**, 8774-8792. (b) J. K. Gregory, D. C. Clary, K. Liu, M. G. Brown and R. J. Saykally, *Science*, 1997, **275**, 814-817. (c) Y. C. Choi, C. Pak and K. S. Kim, *J. Chem. Phys.*, 2006, **124**, 094308-4. (d) T. James and D. J. Wales, *J. Chem. Phys.*, 2007, **126**, 054506-13. (e) J. F. Perez, C. Z. Hadad and A. Restrepo, *Int. J. Quant. Chem.*, 2008, **108**, 1653-1659. (f) D. Rai, A. D. Kulkarni, S. P. Gejji and R. K. Pathak, *J. Chem. Phys.*, 2008, **128**, 034310-14. (g) G. Hincapie, N. Acelas, M. Castaño, J. David and A. Restrepo, *J. Phys. Chem. A*, 2010, **114**, 7809-7814. (h) F. Ramírez, C. Z. Hadad, D. Guerra, J. David and A. Restrepo, *Chem. Phys. Lett.*, 2011, **507**, 229-233.

4 (a) E. Honeggere and S. Leutwyler, *J. Chem. Phys.*, 1987, **88**, 2582-2595. (b) F. Huisken, M. Kaloudis and A. Kulcke, *J. Chem. Phys.*, 1996, **104**, 17-25. (c) J. Kim and K. S. Kim, *J. Chem. Phys.*, 1998, **109**, 5886-5895. (d) M. Losada and S. Leutwyler, *J. Chem. Phys.*, 2002, **117**, 2003-2016. (e) K. Ohno, M. Okimura, N. Akaib and Y. Katsumoto, *Phys. Chem. Chem. Phys.*, 2005, **7** , 3005-3014 (f) Y. Wang and J. M. Bowman, *J. Phys. Chem. Lett.*, 2013, **4**, 1104-1108. (g) A. K. Samanta, L. C. Ch'ng and H. Reisler, *Chem. Phys. Lett.*, 2013, **575**, 1-11. (h) A.

Mukhopadhyay, W. T. S. Cole and R. J. Saykally, *Chem. Phys. Lett.*, 2015, **633**, 13-26.

5 (a) B. E. Rocher-Casterline, L. C. Ch'ng, A. K. Mollner and H. Reisler, *J. Chem. Phys.*, 2011, **134**, 211101-4. (b) L. C. Ch'ng, A. K. Samanta, G. Czakó, J. M. Bowman and H. Reisler, *J. Am. Chem. Soc.*, 2012, **134**, 15430-15435. (c) L. C. Ch'ng, A. K. Samanta, Y. Wang, J. M. Bowman and H. Reisler, *J. Phys. Chem. A*, 2013, **117**, 7207-7216.

6 (a) N. M. Levinson, S. D. Fried and S. G. Boxer, *J. Phys. Chem. B*, 2012, **116**, 10470-10476. (b) S. Bagchi, S. D. Fried and S. G. Boxer, *J. Am. Chem. Soc.*, 2012, **134**, 10373-10376. (c) S. D. Fried, L.-P. Wang, S. G. Boxer, P. Ren and V. S. Pande, *J. Phys. Chem. B*, 2013, **117**, 16236-16248. (d) S. D. Fried, S. Bagchi and S. G. Boxer, *J. Am. Chem. Soc.*, 2013, **135**, 11181-11192. (e) S. D. Fried, S. Bagchi and S. G. Boxer, *Science*, 2014, **346**, 1510-1514. (f) S. D. Fried and S. G. Boxer, *Acc. Chem. Res.*, 2015, **48**, 998-1006.

7 (a) M. Saggu, N. M. Levinson and S. G. Boxer, *J. Am. Chem. Soc.*, 2011, **133**, 17414-17419. (b) M. Saggu, N. M. Levinson and S. G. Boxer, *J. Am. Chem. Soc.*, 2012, **134**, 18986-18997.

8 M. J. Frisch, G. W. Trucks, H. B. Schlegel, G. E. Scuseria, M. A. Robb, J. R. Cheeseman, G. Scalmani, V. Barone, B. Mennucci, G. A. Petersson, H. Nakatsuji, M. Caricato, X. Li, H. P. Hratchian, A. F. Izmaylov, J. Bloino, G. Zheng, J. L. Sonnenberg, M. Hada, M. Ehara, K. Toyota, R. Fukuda, J. Hasegawa, M. Ishida, T. Nakajima, Y. Honda, O. Kitao, H. Nakai, T. Vreven, J. A. Montgomery, Jr., J. E. Peralta, F. Ogliaro, M. Bearpark, J. J. Heyd, E. Brothers, K. N. Kudin, V. N. Staroverov, R. Kobayashi, J. Normand, K. Raghavachari, A. Rendell, J. C. Burant,

S. S. Iyengar, J. Tomasi, M. Cossi, N. Rega, J. M. Millam, M. Klene, J. E. Knox, J. B. Cross, V. Bakken, C. Adamo, J. Jaramillo, R. Gomperts, R. E. Stratmann, O. Yazyev, A. J. Austin, R. Cammi, C. Pomelli, J. W. Ochterski, R. L. Martin, K. Morokuma, V. G. Zakrzewski, G. A. Voth, P. Salvador, J. J. Dannenberg, S. Dapprich, A. D. Daniels, O. Farkas, J. B. Foresman, J. V. Ortiz, J. Cioslowski and D. J. Fox, *Gaussian-09, Revision A.02* Gaussian, Inc., Wallingford CT, 2009.

9 GaussView, Version 5, D. Roy; K. Todd and M. John, Semichem Inc., Shawnee Mission, KS, 2009.

10 (a) P. Politzer and D. G. Truhlar, *Chemical Applications of Atomic and Molecular Electrostatic Potentials*, Springer Science+Business Medis, Plenum Press, New York, 1981. (b) Johnson, B. G.; Gill, P. M. W.; Pople, J. A.; Fox, D. *Chem. Phys. Lett.*, 1993, **206**, 239-246. (c) S. R. Gadre and R. N. Shirsat, *Electrostatics of Atoms and Molecules*, University Press: Hyderabad, India, 2000. (d) N. Mohan, C. H. Suresh, *J. Phys. Chem. A*, 2014, **118**, 1697-1705.

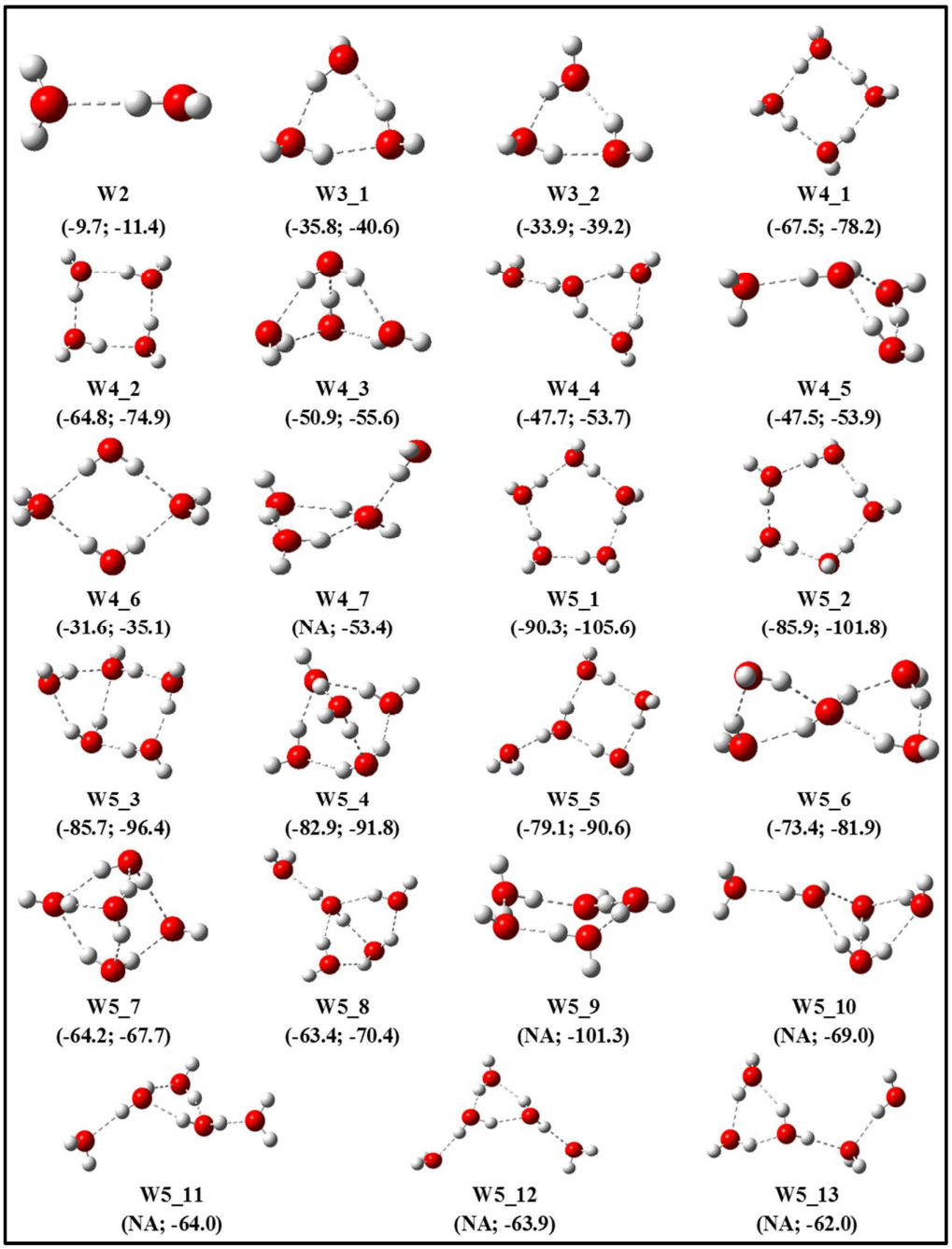

Fig. 1. Optimized structures of water –dimer, –trimer, –tetramer and –pentamer. The calculated stabilization energies are at MP2/aug-cc-pVDZ and B3LYP/6-311++G(*d,p*) levels of theory are shown in parenthesis. NA indicates that the structure is not a stable minimum at a given level of theory.

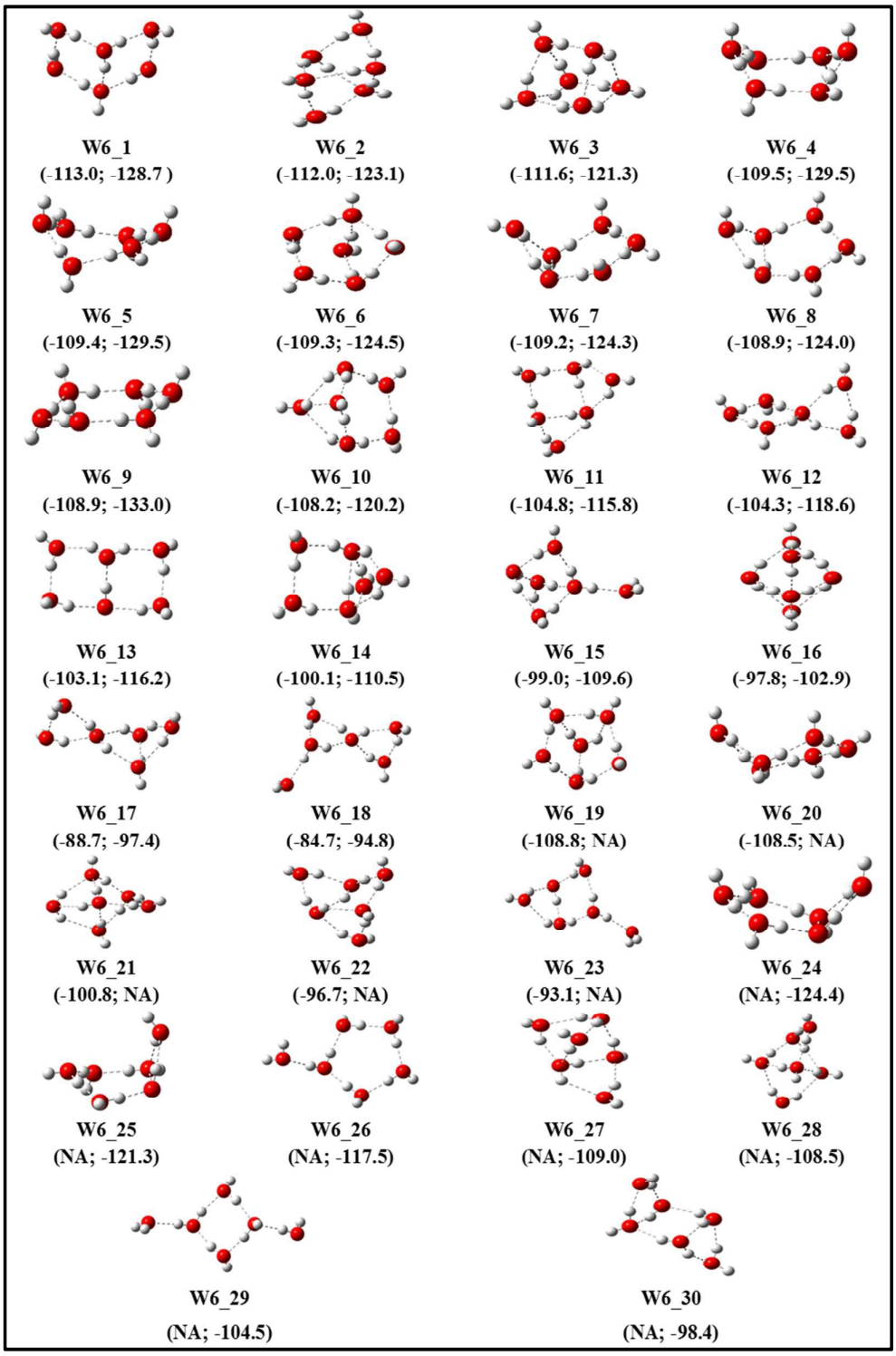

Fig. 2. Optimized structures of water–hexamer. The calculated stabilization energies are at MP2/aug-cc-pVDZ and B3LYP/6-311++G(*d,p*) levels of theory are shown in parenthesis. NA indicates that the structure is not a stable minimum at a given level of theory.

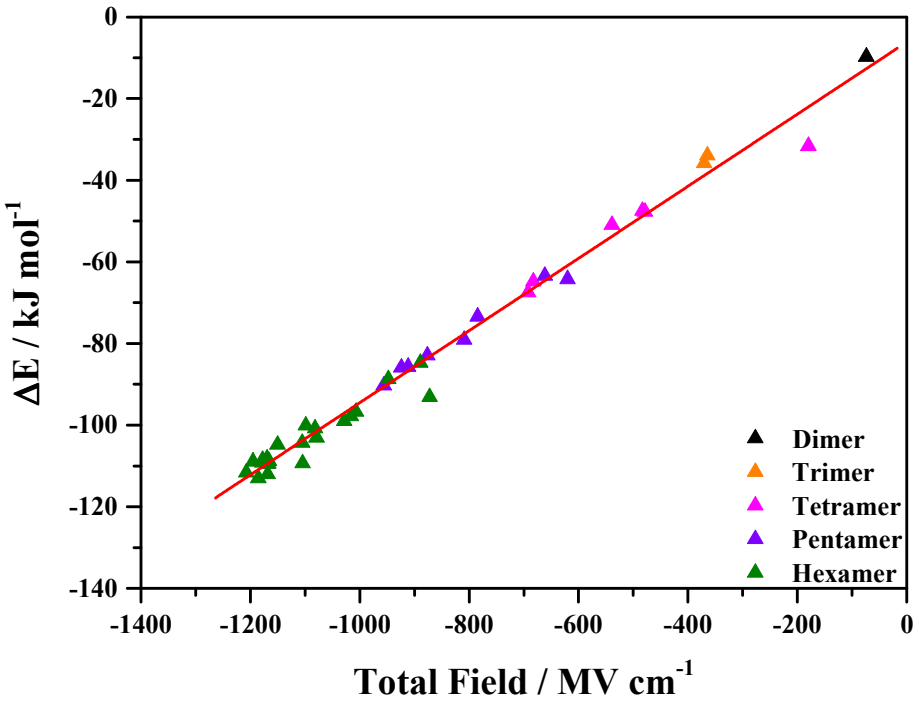

Fig. 3. Plot of total stabilization energy against total electric field calculated at MP2/aug-cc-pVDZ level for several water clusters. The straight line is a linear fit (R^2 = 0.987) to the data points.

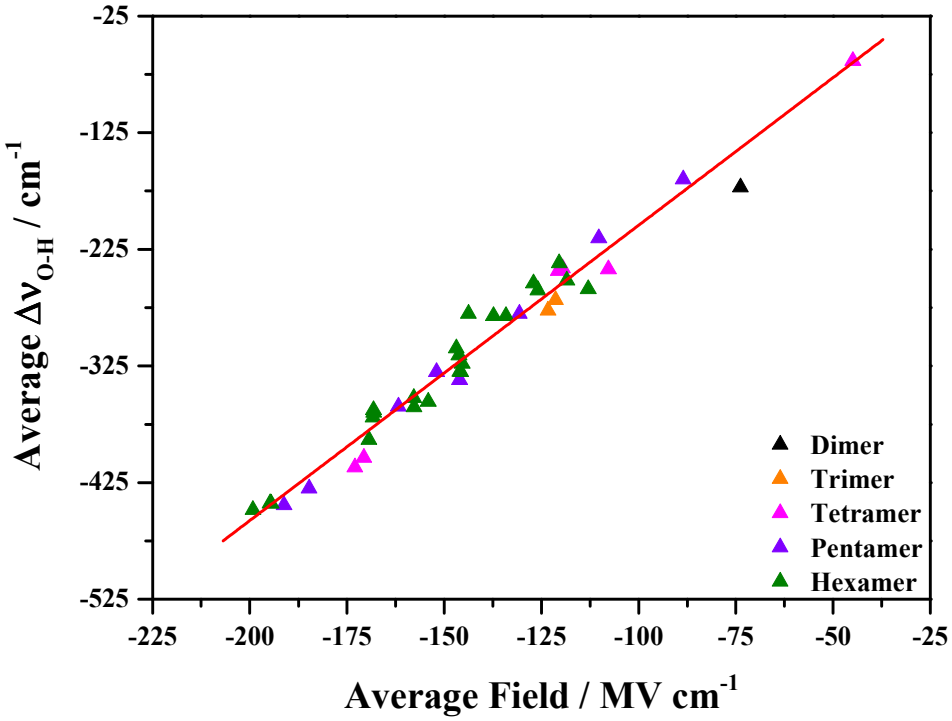

Fig. 4. Plot of average red-shift in the O–H stretching frequencies against average electric field calculated at MP2/aug-cc-pVDZ level for several water clusters. The straight line is a linear fit (R^2 = 0.971) to the data points, which corresponds to the Stark tuning rate of 2.53 cm^{-1}/(MV cm^{-1}).

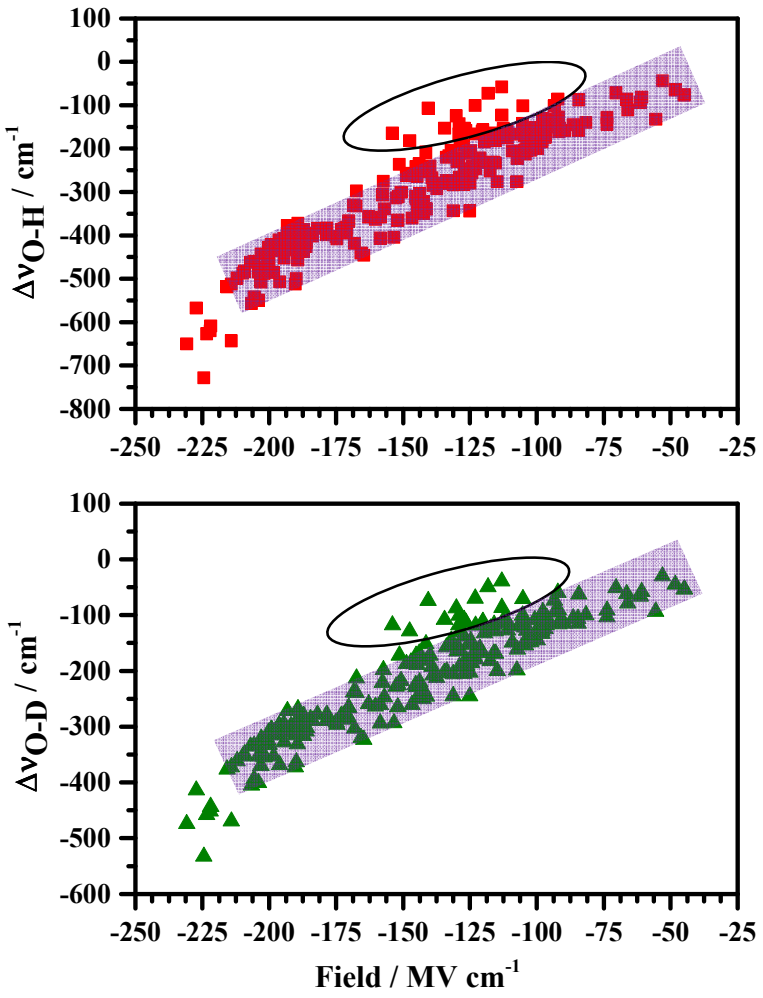

Fig. 3. Plot of red-shift in the O–H (squares) and O–D (triangles) stretching frequencies against the corresponding electric field calculated at MP2/aug-cc-pVDZ level for several water clusters. The shaded region indicates linear trend with ± 100 cm^{-1} deviations. Data points in the encircled region and data points with fields above 200 MV cm^{-1} show larger deviations from linearity.

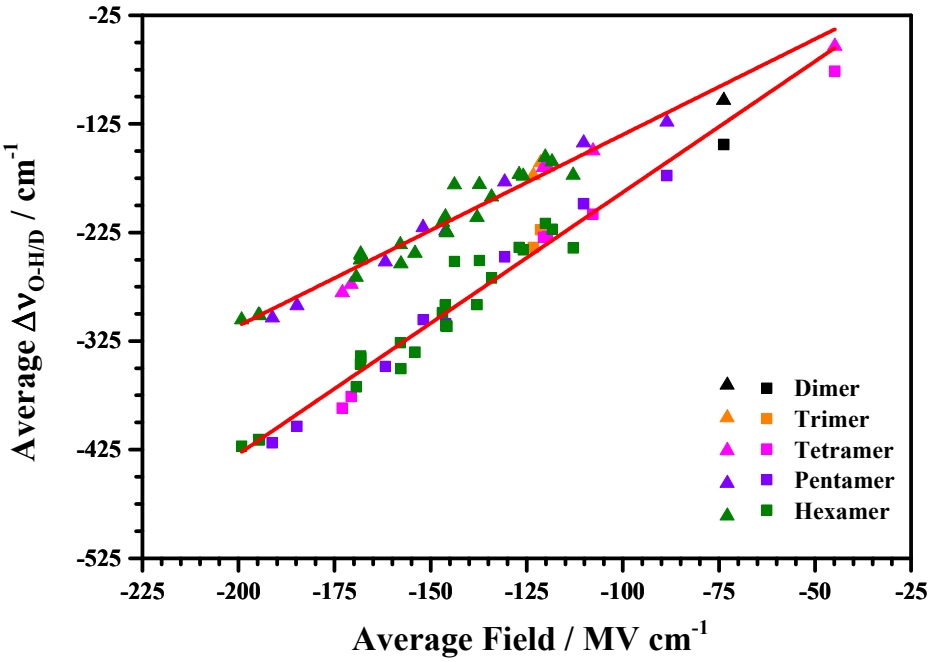

Fig. 7. Plot of average red-shift in the O–D (Triangles) and O–H (Squares) stretching frequencies against average electric field calculated at MP2/aug-cc-pVDZ level for several water clusters. The straight lines are linear fits to the data points with R^2 values of 0.963 and 0.965 and the corresponding Stark tuning rates are 1.76 and 2.41 cm^{-1}/(MV cm^{-1}) for O–D and O–H stretches, respectively.

Table 1. ZPE and BSSE corrected stabilization energies (kJ mol^{-1}), average hydrogen bond energy (kJ mol^{-1}) and total field (MV cm^{-1}) for the water clusters W_n (n = 2−6) calculated at various levels of theory

Structure	No. of H-bond	Avg. H bond Energy		Stabilization energy		Total Field	
		MP2 aug-cc-pVDZ	B3LYP 6-311++G(d,p)	MP2 aug-cc-pVDZ	B3LYP 6-311++G(d,p)	MP2 aug-cc-pVDZ	B3LYP 6-311++G(d,p)
W2	1	-9.7	-11.4	-9.7	-11.4	-73.79	-81.79
W3_1	3	-11.9	-13.5	-35.8	-40.6	-369.92	-392.72
W3_2	3	-11.3	-13.1	-33.9	-39.2	-364.17	-387.00
W4_1	4	-16.9	-19.6	-67.5	-78.2	-692.00	-719.13
W4_2	4	-16.2	-18.7	-64.8	-74.9	-682.73	-710.48
W4_3	5	-10.2	-11.1	-50.9	-55.6	-538.84	-555.65
W4_4	4	-11.9	-13.4	-47.7	-53.7	-478.33	-503.50
W4_5	4	-11.9	-13.5	-47.5	-53.9	-482.72	-506.30
W4_6	4	-7.9	-8.8	-31.6	-35.1	-179.51	-194.40
W4_7	4	---	-13.4	---	-53.4	---	-493.85
W5_1	5	-18.1	-21.1	-90.3	-105.6	-955.94	-992.22
W5_2	5	-17.2	-20.4	-85.9	-101.8	-923.92	-972.84
W5_3	6	-14.3	-16.1	-85.7	-96.4	-911.72	-941.97
W5_4	6	-13.8	-15.3	-82.9	-91.8	-876.19	-892.74
W5_5	5	-15.8	-18.1	-79.1	-90.6	-808.91	-837.66
W5_6	6	-12.2	-13.7	-73.4	-81.9	-784.30	-814.69
W5_7	7	-9.2	-9.7	-64.2	-67.7	-619.86	-633.93
W5_8	6	-10.6	-11.7	-63.4	-70.4	-661.47	-680.70
W5_9	5	---	-20.3	---	-101.3	---	-973.14
W5_10	6	---	-11.5	---	-69.0	---	-658.73
W5_11	5	---	-12.8	---	-64.0	---	-584.67
W5_12	5	---	-12.8	---	-63.9	---	-580.51
W5_13	5	---	-12.4	---	-62.0	---	-537.00
W6_1	7	-16.1	-18.4	-113.0	-128.7	-1185.34	-1215.54
W6_2	8	-14.0	-15.4	-112.0	-123.1	-1168.08	-1182.39
W6_3	9	-12.4	-13.5	-111.6	-121.3	-1207.13	-1210.07

W6_4	6	-18.3	-21.6	-109.5	-129.5	-1168.43	-1222.22
W6_5	6	-18.2	-21.6	-109.4	-129.5	-1167.08	-1223.46
W6_6	7	-15.6	-17.8	-109.3	-124.5	-1104.29	-1190.62
W6_7	7	-15.6	-17.8	-109.2	-124.3	-1178.10	-1214.99
W6_8	7	-15.6	-17.7	-108.9	-124.0	-1176.83	-1215.89
W6_9	6	-18.2	-22.2	-108.9	-133.0	-1195.03	-1239.57
W6_10	8	-13.5	-15.0	-108.2	-120.2	-1169.66	-1197.17
W6_11	8	-13.1	-14.5	-104.8	-115.8	-1150.37	-1172.39
W6_12	7	-14.9	-16.9	-104.3	-118.6	-1105.15	-1134.93
W6_13	7	-14.7	-16.6	-103.1	-116.2	-1078.77	-1118.18
W6_14	8	-12.5	-13.8	-100.1	-110.0	-1098.37	-1105.99
W6_15	7	-14.1	-15.7	-99.0	-109.6	-1028.35	-1034.71
W6_16	9	-10.9	-11.4	-97.8	-102.9	-1016.36	-1007.22
W6_17	8	-11.1	-12.2	-88.7	-97.4	-947.61	-971.33
W6_18	7	-12.1	-13.5	-84.7	-94.8	-889.10	-920.53
W6_19	8	-13.6	---	-108.8	---	-1166.09	---
W6_20	7	-15.5	---	-108.5	---	-1177.30	---
W6_21	9	-11.2	---	-100.8	---	-1081.64	---
W6_22	8	-12.1	---	-96.7	---	-1007.08	---
W6_23	7	-13.3	---	-93.1	---	-965.64	---
W6_24	7	---	-17.8	---	-124.4	---	-1216.44
W6_25	7	---	-17.3	---	-121.3	---	-1195.31
W6_26	6	---	-19.6	---	-117.5	---	-1106.21
W6_27	8	---	-13.6	---	-109.0	---	-1106.05
W6_28	8	---	-13.6	---	-108.5	---	-991.14
W6_29	6	---	-17.4	---	-104.5	---	-948.86
W6_30	8	---	-12.3	---	-98.4	---	-928.46